ACS OMEGA

Article

Cite This: ACS Omega 2019, 4, 6923−6930

http://pubs.acs.org/journal/acsodf

Yellow Persistent Phosphor $Ba_{13.35}Al_{30.7}Si_{5.3}O_{70}:Eu^{2+},Tm^{3+}$ from the Energy Regulation of Rare-Earth Ions

Haijing Jiang,[†] Yonglei Jia,*[,‡] Tianliang Qu,*[,‡] Yao Pan,[‡] Kaiyong Yang,[‡] and Hui Luo[‡]

[†]State Key Laboratory of Inorganic Synthesis and Preparative Chemistry, Jilin University, 2699 Qianjin Street, Changchun 130012, P. R. China

[‡]Department of Photoelectric Engineering, College of Advanced Interdisciplinary Studies, National University of Defense Technology, Changsha, Hunan 410073, P. R. China

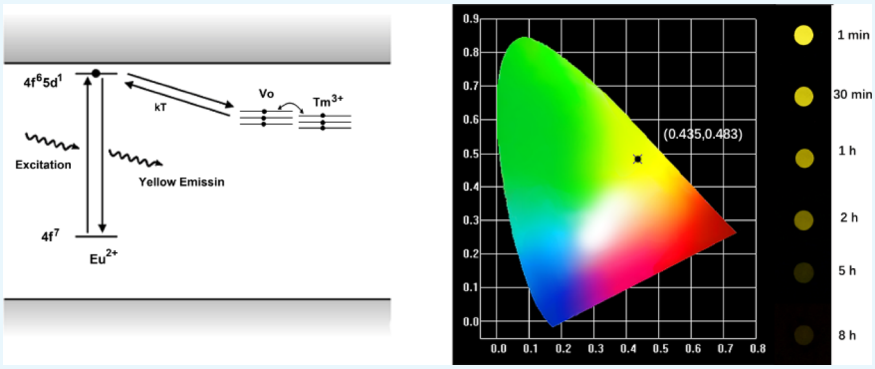

ABSTRACT: The luminescence properties of $Ba_{13.35}Al_{30.7}Si_{5.3}O_{70}:Eu^{2+}$ and $Ba_{13.35}Al_{30.7}Si_{5.3}O_{70}:Eu^{2+},Tm^{3+}$ phosphors are presented. After being excited by a light source, $Ba_{13.35}Al_{30.7}Si_{5.3}O_{70}:Eu^{2+},Tm^{3+}$ phosphors emit intense yellow long persistent luminescence covering the region from 450 to 700 nm, which can last about 8 h. Thermoluminescence curves were demonstrated to analyze the trapping nature of persistent luminescence. Tm^{3+} is added to improve the long persistent luminescence properties of phosphors. The mechanism of persistent luminescence has been studied.

INTRODUCTION

Long persistent luminescence phosphors can store light energy and release the storage of energy at a certain temperature with long-lasting visible light emission.[1] After the removal of light source, a persistent luminescence material can continue to emit persistent luminescence from minutes to hours, which currently has been applicable or researchable in the field of night illumination, optical storage, and solar energy utilization.[2−5] In recent years, nanoparticles with near-infrared (NIR) persistent luminescence have emerged as a new class of background-free contrast agents that are promising for in vivo imaging techniques.[6−9]

Alkaline earth silicate and aluminate are favorable host materials. The development and research of rare-earth ion sensitized aluminate and silicate materials has been the principal part of long persistent luminescence materials in the recent years.[10,11] Aluminosilicate is also a good luminescent matrix with advantages such as stable chemical property, low synthesis temperature, abundant raw material, and low cost. Therefore, aluminosilicate has great value in research and application as a novel long persistent luminescence matrix. The structure of aluminosilicate is complicated, with a wide variety of phase compositions. Thus, it is difficult to prepare a single pure phase. The complex crystal structure of aluminosilicate can create multiple lattice environments for doped rare-earth ions, which can generate different luminescence centers, therefore obtaining a unique luminescence property.[12,13] However, until now, only a few aluminosilicate luminescent materials have been reported, such as $BaAl_2Si_2O_8$ and $CaAl_2Si_2O_8$.[14,15]

We use $Ba_{13.35}Al_{30.7}Si_{5.3}O_{70}$ (BASO) as the matrix, and by doping the Eu^{2+} ion, the yellow luminescence material $Ba_{13.35}Al_{30.7}Si_{5.3}O_{70}:Eu^{2+}$ is obtained. After adding the Tm^{3+} ion, $Ba_{13.35}Al_{30.7}Si_{5.3}O_{70}:Eu^{2+},Tm^{3+}$ shows an excellent persistent luminescence property. By measuring and analyzing the sample, we study the photoluminescence property and persistent luminescence property of $Ba_{13.35}Al_{30.7}Si_{5.3}O_{70}:Eu^{2+}$ and $Ba_{13.35}Al_{30.7}Si_{5.3}O_{70}:Eu^{2+},Tm^{3+}$ systematically.

RESULTS AND DISCUSSION

Phase Identification and Crystal Structure. $Ba_{13.35}Al_{30.7}Si_{5.3}O_{70}$ belongs to a hexagonal crystal system, with space group $P6_3/m$ (Figure 1a). The lattice parameters are $a = b = 1.5178$ nm, $c = 0.8871$ nm, $\alpha = \beta = 90°$, $\gamma = 120°$, and $V = 1.7696$ nm^3.[16] In the lattice of BASO, AlO_4 and Al/SiO_4 tetrahedra form a three-dimensional network structure by

Received: January 20, 2019
Accepted: March 7, 2019
Published: April 16, 2019

DOI: 10.1021/acsomega.9b00180
ACS Omega 2019, 4, 6923−6930

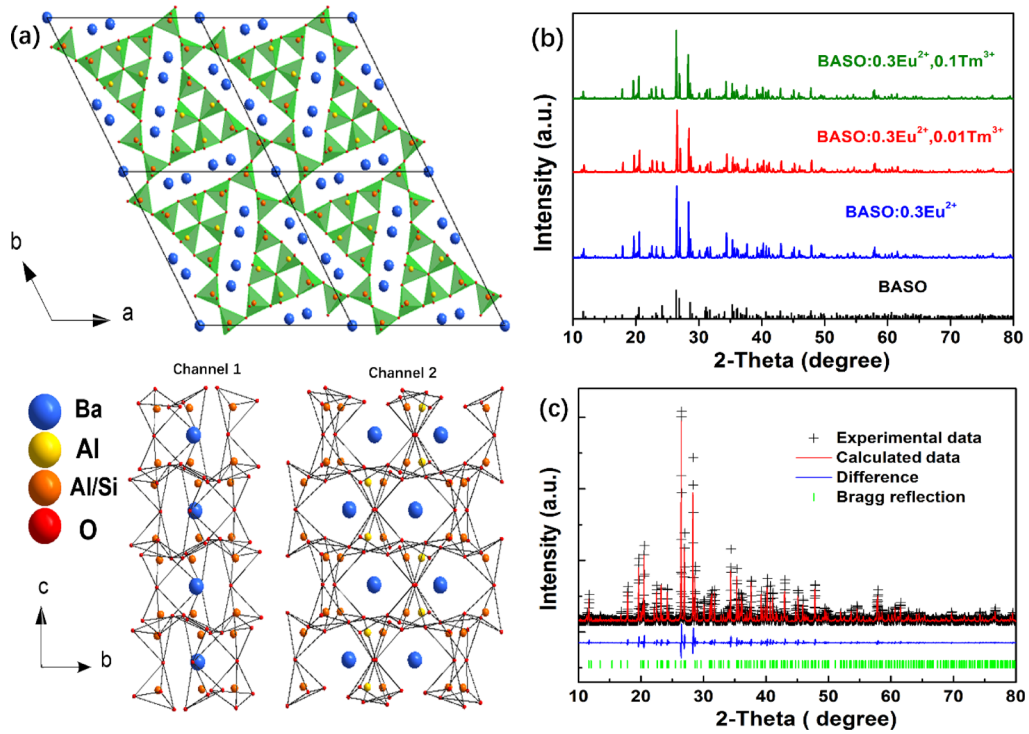

Figure 1. (a) Crystal structure diagram of $Ba_{13.35}Al_{30.7}Si_{5.3}O_{70}$. (b) XRD patterns of the typically prepared phosphors. The standard data for $Ba_{13.35}Al_{30.7}Si_{5.3}O_{70}$ are shown as references. (c) Powder X-ray diffraction refinement of $Ba_{12.95}Al_{30.7}Si_{5.3}O_{70}$:$0.3Eu^{2+}$,$0.1Tm^{3+}$.

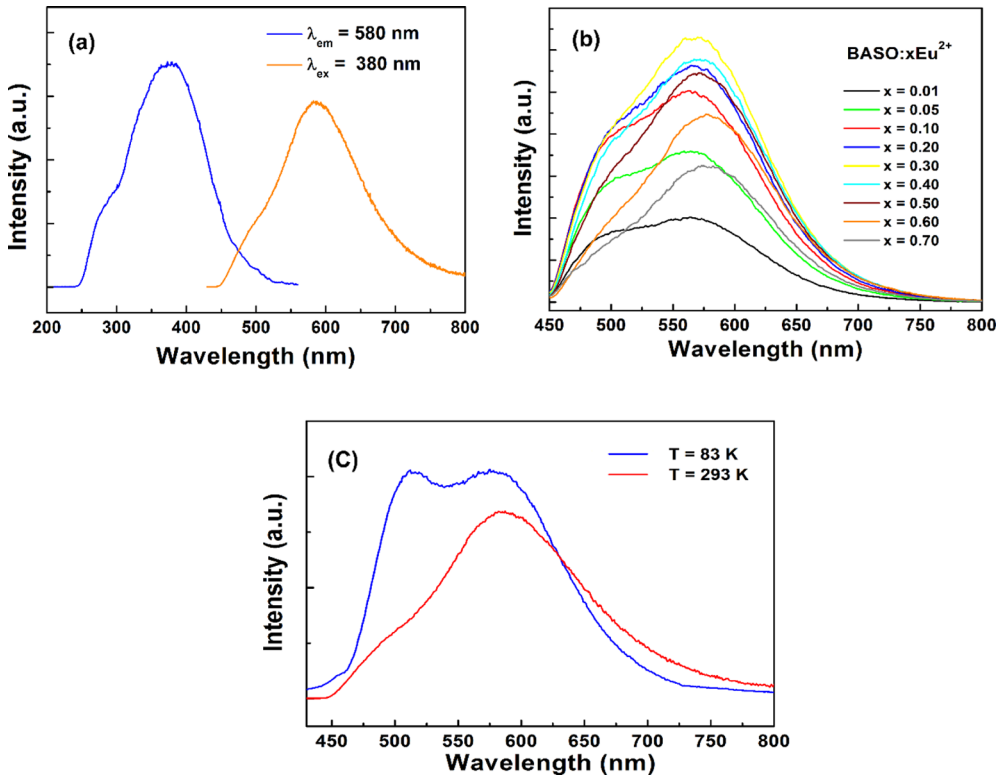

Figure 2. (a) PL and PLE spectra of BASO:$0.3Eu^{2+}$. (b) Emission spectra of BASO:xEu^{2+}. (c) Emission spectra of BASO:$0.3Eu^{2+}$ at room temperature and low temperature.

means of a sharing vertex. Along the direction of the *c* axis, a three-dimensional network structure of AlO_4 and Al/SiO_4 tetrahedra forms two kinds of channels. In the lattice, there are three kinds of Ba lattice sites. There are two lattice sites, Ba(1) and Ba(3), which occupy completely in channel 2. Channel 1 is occupied by the Ba(2) lattice site, which consists of a six-membered ring formed by six Al/SiO_4 tetrahedra. The Ba(1) lattice site in channel 2 and Ba(1) or Ba(3) lattice sites in channel 1 can be connected by either the Al/SiO_4 tetrahedron or the O atom directly (Ba−O−Ba). The

DOI: 10.1021/acsomega.9b00180
ACS Omega 2019, 4, 6923−6930

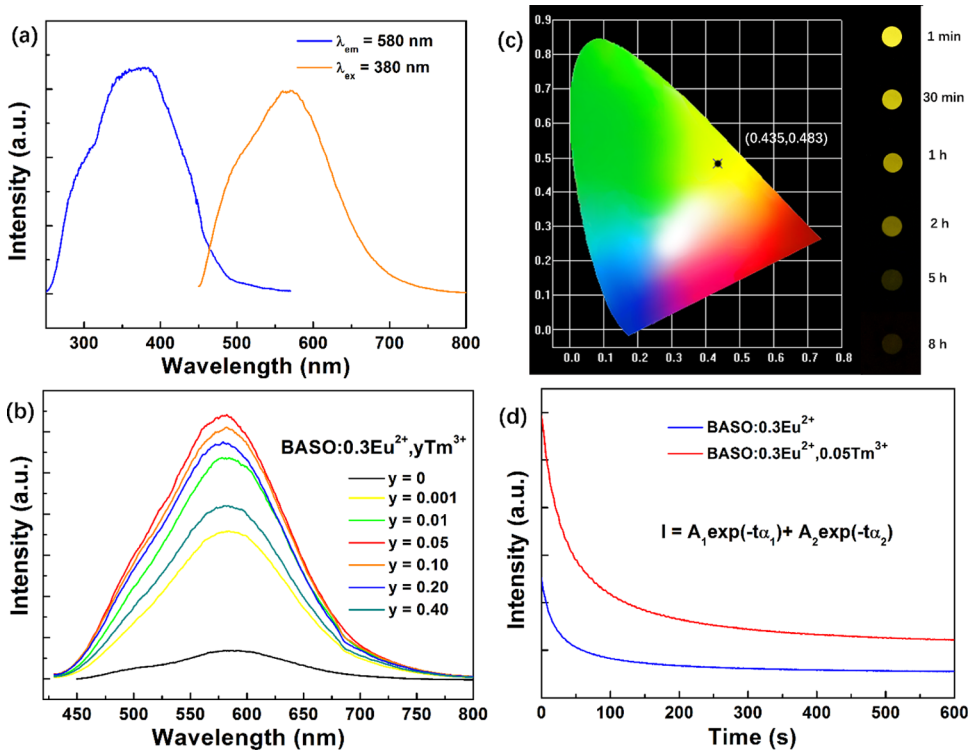

Figure 3. (a) PL and PLE spectra of BASO:0.3Eu^{2+},0.1Tm^{3+}. (b) Persistent luminescence spectrum of BASO:0.3Eu^{2+},$x$$Tm^{3+}$. (c) CIE coordinates of BASO:0.3Eu^{2+},0.1Tm^{3+} phosphor and the long persistent images of the BASO:0.3Eu^{2+},0.1Tm^{3+} phosphor taken after sunlight activation for 30 min. (d) Persistent luminescence decay curves of BASO:0.3Eu^{2+} and BASO:0.3Eu^{2+},0.05Tm^{3+}.

coordination number of the Ba^{2+} ion and oxygen atom in channel 2 is 9. The ionic radius is 0.142 nm. The ionic radii of eight-coordinated Eu^{2+} and Tm^{3+} are 0.125 and 0.0994 nm, respectively. The ionic radii of nine-coordinated Eu^{2+} and Tm^{3+} are 0.13 and 0.1052 nm, respectively. In the lattice of BASO:Eu^{2+},Tm^{3+}, the ionic radius of Eu^{2+} is close to Tm^{3+} and Ba^{2+}. Eu^{2+} and Tm^{3+} ions tend to substitute the lattice site of Ba^{2+} in the matrix. Figure 1b shows the X-ray diffraction pattern of BASO:Eu^{2+},Tm^{3+}. The XRD diffraction peaks are in accordance with BASO, which indicate that Eu^{2+} and Tm^{3+} enter the lattice successfully.

To understand the crystal structure information of the co-doped sample, we refer to the BASO crystal structure information reported by Rief et al.[16] We proceed to the BASO:0.3Eu^{2+},0.1Tm^{3+} structure refinement using GSAS software, as shown in Figure 1c. After the refinement, the crystal structure information is $a = b = 1.5058$ nm, $c = 0.8732$ nm, $\alpha = \beta = 90°$, $\gamma = 120°$, and $V = 1.7146$ nm^3. From the results of refining, cell parameters can be seen, and the unit cell volume of BASO:0.3Eu^{2+},0.1Tm^{3+} decreases. The reason for this phenomenon may be the substitution of the Ba^{2+} ion with a larger ionic radius by Eu^{2+} and Tm^{3+} with smaller ionic radii. $Tm_{Ba}^{\bullet}$ defect with a positive charge is generated after the substitution of the trivalent Tm^{3+} ion. At the same time, Ba^{2+} ionic vacancy V_{Ba}'' is formed to keep the charge balance of the lattice. These parameters cause the shrinkage of the unit cell volume. Therefore, it proves that Eu^{2+} and Tm^{3+} have already entered the BASO lattice side-on.

Luminescence Property of the Single-Doped Sample BASO:Eu^{2+}. Figure 2a represents the photoluminescence (PL) and photoluminescence excitation (PLE) spectra of BASO:0.3Eu^{2+}. By the excitation of 380 nm ultraviolet light, the sample BASO:0.3Eu^{2+} shows intense yellow fluorescence. The PL spectrum consists of the asymmetric broad band with the main emission peak located at 580 nm and the wavelength ranging from 450 to 750 nm, which belongs to the allowed transition of $4f^6 5d^1 \rightarrow 4f^7$.[11] BASO:0.3$Eu^{2+}$ can also be excited by a light source with the wavelength ranging from 250 to 520 nm, corresponding to $4f^7 \rightarrow 4f^6 5d^1$ that allowed the transition of Eu^{2+}.[17] The PL spectrum of BASO:0.3Eu^{2+} consists of the main emission peak located at 580 nm and a broad peak located at 500 nm. The emission spectrum of BASO:0.3Eu^{2+} may be the combination of multiple emission light of the Eu^{2+} ion. The position and intensity of the emission wavelength located at different lattice sites are different. Therefore, the asymmetric emission peak of BASO:0.3Eu^{2+} is generated. In the matrix with multiple crystal lattice sites, Eu^{2+} is usually preferred to occupy the easily substituted Ba^{2+} ion site.[18] With the increase in Eu^{2+} ionic concentration, the occupied lattice sites will change. The PL spectra of samples with different doping concentrations are shown in Figure 2b.

Obviously, with the increase in Eu^{2+} doping concentration, the shape of the BASO:$x$$Eu^{2+}$ emission spectral curve varies greatly. The BASO:$x$$Eu^{2+}$ emission spectra consist of two emission peaks located at 500 and 580 nm. The intensities of the two emission peaks are close. With the increase in Eu^{2+} ionic concentration, the intensities of emission peaks located at 500 and 580 nm increase simultaneously. The intensity difference of the two emission peaks becomes larger and larger to the extent that we can only observe one main emission peak located at 580 nm in the emission spectrum of BASO:0.7Eu^{2+}. To research the luminescence characteristics of Eu^{2+} in the BASO:Eu^{2+} material, we test the low-temperature excitation and emission spectra. In the state of low temperature, the lattice vibration and the energy exchange between Eu^{2+} ions have a small influence on the transition emission of

DOI: 10.1021/acsomega.9b00180
ACS Omega 2019, 4, 6923−6930

luminescent ions, which, to some extent, can separate the emission spectra of luminescent ions located at different lattice sites. In Figure 2c, the emission spectrum of BASO:0.3Eu^{2+} in room temperature consists of a main emission peak and a weak peak located at 500 nm. Obviously, in a low temperature of 83 K, the emission spectra of BASO:0.3Eu^{2+} consist of two emission peaks located at 505 and 580 nm, whose intensities are close. This indicates that two kinds of Eu^{2+} ionic luminescence center exist in BASO:Eu^{2+}, whose emission peaks are located at 500 and 580 nm. According to Van Uitert theory, we can assume that the 5d orbital energy level of the Eu^{2+} ion in the same material is mainly affected by the surrounding atom coordination number. In the BASO:Eu^{2+} material, the Eu^{2+} ion has only two coordination numbers (8 and 9). Thus, two different emission wavelengths can possibly be produced. For this purpose, we analyze the luminescence characteristics of Eu^{2+} ions located at different lattice sites with the following equation[19]

$$E = Q[1 - (V/4)^{1/V} 10^{-nE_a r/80}] \quad (1)$$

where E is the position of the Eu^{2+} emission peak, whose unit is cm^{-1}, Q is the Eu^{2+} energy level difference between d orbital and 4f orbital for the free ion, V is the valence of the activated ion (Eu^{2+}), E_a is the electronic affinity of the coordination atom, n is the coordination number of the activated ion, and r is the radius of the matrix cation substituted by the Eu^{2+} ion. For the BASO:Eu^{2+} material, the coordination atom O is affected by SiO_4 and AlO_4 together. The value of E_a will change. According to the equation above, in the situation of the same E_a value, when n is larger, the value of E is larger, and the corresponding emission wavelength is smaller. Therefore, the emission peak at 580 nm should be generated by the eight-coordinated Eu^{2+} ion. Therefore, we can estimate the value of the affinity energy of O in the material according to the emission peak at 580 nm (the activated ion is Eu^{2+}, Q = 34,000 cm^{-1}, V = 2, the coordination number of Ba is 8, r = 0.142 nm, $E \approx$ 17,241.4 cm^{-1}, and calculated E_a = 1.50 eV). We substitute the calculated E_a into the equation (the ionic coordination number of Ba is 9, r = 0.147 nm), and $E \approx$ 20,284.0 cm^{-1} is obtained, which corresponds to the 500 nm emission peak position of the BASO:Eu^{2+} emission spectrum. This explains that there are two kinds of Eu^{2+} ion luminescent center in the material. The 500 and 580 nm emission peaks in the emission spectrum correspond to the nine-coordinated and eight-coordinated Eu^{2+} ion luminescent center, respectively.

Luminescence Property of BASO:Eu^{2+},Tm^{3+}. Figure 3a provides the excitation and emission spectra of the sample BASO:0.3Eu^{2+},0.1Tm^{3+}. By the excitation of 365 nm ultraviolet light, the sample BASO:0.3Eu^{2+},0.1Tm^{3+} can emit intense yellow luminescence as well. The emission spectrum is a broad-band spectrum ranging from 450 to 470 nm, which belongs to the $4f^6 5d^1 \rightarrow 4f^7$ transition emission of Eu^{2+}. The emission spectrum includes two emission peaks, which are the main emission peak located at 580 nm and the weak emission peak located at 500 nm. The co-doped sample is synthesized in the reducing condition. Eu^{3+} has been reduced to Eu^{2+} (no 4f $\rightarrow$ 4f characteristic transition emission peak of Eu^{3+} observed around 610 nm).[20] The added Tm^{3+} ion is difficult to be reduced; therefore, it still exists in a trivalent ion form.[21] There is no characteristic emission peak of the Tm^{3+} ion in the emission spectrum of BASO:0.3Eu^{2+},0.1Tm^{3+}. Thus, in the co-doped sample, Tm^{3+} acts mainly as the assistant activating agent rather than the luminescent center. The two emission peak positions of BASO:0.3Eu^{2+},0.1Tm^{3+} are the same as the emission peak position of BASO:0.3Eu^{2+}, which indicates that the crystal environment of the Eu^{2+} luminescent center does not change much after the Tm^{3+} ion is involved. As shown in Figure 3a, BASO:0.3Eu^{2+},0.1Tm^{3+} can also be excited by the light with the wavelength from 250 to 520 nm, belonging to the $4f^7 \rightarrow 4f^6 5d^1$ transition of Eu^{2+}. This declares that the sample can be activated by ultraviolet and blue light-emitting diode (LED) chips, which is very important for the application of long persistent luminescence materials.

We use near ultraviolet light or sunlight to irradiate BASO:Eu^{2+},Tm^{3+} for some time. We can observe strong yellow persistent luminescence in a dark room after the removal of light source. The sample is irradiated under a 460 nm blue light source for 1 min. The persistent luminescence spectra were tested after removing the light source for 10 s, as shown in Figure 3b. The persistent luminescence spectrum of BASO:0.3Eu^{2+},$x$$Tm^{3+}$ is in accordance with its PL spectrum. Therefore, the persistent luminescence of BASO:Eu^{2+},Tm^{3+} derives from the $4f^6 5d^1 \rightarrow 4f^7$ transition of Eu^{2+}. Figure 3c shows the CIE chromaticity coordinates of the persistent luminescence of BASO:Eu^{2+},Tm^{3+}, and the persistent luminescence can last for 8 h. We observe that BASO:0.3Eu^{2+} can also emit yellow persistent luminescence without adding the Tm^{3+} ion; however, the intensity is weak. The persistent luminescence intensity of the sample improves much after adding Tm^{3+}. With the further increase in Tm^{3+} concentration, the persistent luminescence intensity of the sample increases gradually. However, when the Tm^{3+} concentration is above 0.1, the persistent luminescence intensity of the sample decreases. This indicates that the addition of Tm^{3+} changes the trap distribution of the material and improves the energy storage ability of the materials. With the addition of Tm^{3+} ions, the amount of traps increases in the materials. The persistent luminescence intensity increases therewith. When Tm^{3+} reaches a certain concentration, the co-doped ions cause concentration quenching with the addition of the doped concentration, which decreases the persistent luminescence intensity.

Figure 3d shows the persistent luminescence decay curves of BASO:0.3Eu^{2+} and BASO:0.3Eu^{2+},0.05Tm^{3+}. BASO:0.3Eu^{2+} possesses quite low initial persistent luminescence intensity and will soon decay to the lower level. The co-doped BASO:0.3Eu^{2+},Tm^{3+} sample possesses a higher initial persistent luminescence intensity. After decaying to a certain intensity level, the decay of persistent luminescence becomes quite slow. Thus, it can emit persistent luminescence for a long time. To study the decay regularity of persistent luminescence, we fit the decay curves of BASO:0.3Eu^{2+} and BASO:0.3Eu^{2+},0.05Tm^{3+} and find that the decay of persistent luminescence in accordance with the second-order kinetic attenuation rule[22−24]

$$I = A_1 \exp(-t\alpha_1) + A_2 \exp(-t\alpha_2) \quad (2)$$

where I is the persistent luminescence intensity of the sample, A_1 and A_2 are the constants, and α_1 and α_2 represent the decay constants, which reflect the decay rate to some extent. To the sample BASO:0.3Eu^{2+}, α_1 = 0.0575 and α_2 = 0.0086. To the sample BASO:0.3Eu^{2+},0.1Tm^{3+}, α_1 = 0.0413 and α_2 = 0.0042. It can thus be seen that the numerical value of α_1 and α_2 to the co-doped sample BASO:0.3Eu^{2+},0.05Tm^{3+} is smaller than BASO:0.3Eu^{2+}, which indicates that the Tm^{3+} ion not only

DOI: 10.1021/acsomega.9b00180
ACS Omega 2019, 4, 6923−6930

improves the persistent luminescence intensity of BASO: Eu^{2+} but also decreases the persistent luminescence decay rate.

Thermoluminescence Spectra of the Sample. In the long-lasting phosphor activated by Eu^{2+}, co-doped trivalent rare-earth ions are frequently non-luminescent. Instead, they store energy as a trap center and gradually release the energy at the function of temperature. They transmit the energy to the Eu^{2+} luminescent center to generate persistent luminescence. The intensity of persistent luminescence and the time of duration are frequently decided by the existing state of the trap. To research the generating process of the persistent luminescence and the function of Tm^{3+} in BASO:Eu^{2+},Tm^{3+}, we test the three-dimensional thermoluminescence spectra of the sample.

Figure 4a shows the three-dimensional thermoluminescence spectra of BASO:0.3Eu^{2+},0.1Tm^{3+}. The *X* axis represents the luminescence wavelength. The *Y* axis represents the temperature. *Z* axis represents the intensity of thermoluminescence. The *XZ* plane is the thermoluminescence spectra of the sample at different temperatures and the persistent luminescence emission spectra at one temperature. The *YZ* plane is the relationship curve of the temperature and emission intensity monitoring at one temperature. Converting the three-dimensional thermoluminescence spectra of BASO:0.3Eu^{2+},0.1Tm^{3+} to the two-dimensional thermoluminescence curve about the emission intensity and temperature using software, we obtain Figure 4b. We use thermoluminescence analysis software to deal with the two-dimensional thermoluminescence curve of the sample BASO:0.3Eu^{2+},0.1Tm^{3+}. We obtain the relative parameters of thermoluminescence by software fitting of the curves. Because of the uncertainty of the thermoluminescence dynamic series, the theory we use to fit is based on the general dynamic series calculation equation:[25]

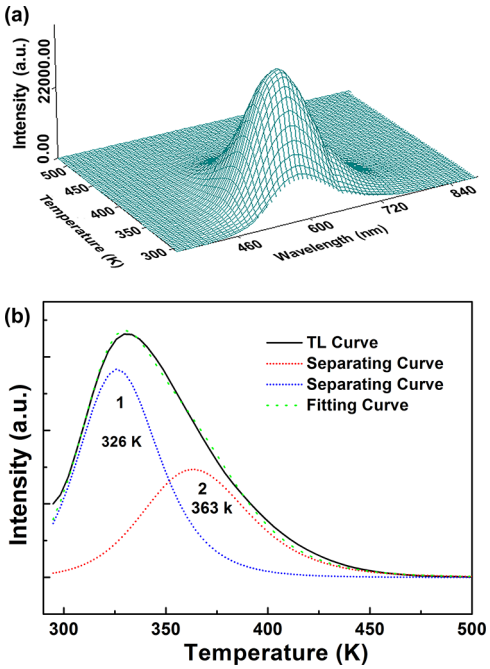

Figure 4. (a) Three-dimensional thermoluminescence spectra of BASO:0.3Eu^{2+},0.1Tm^{3+}. (b) Two-dimensional thermoluminescence curves.

$$I(T) = sn_0 \times \exp\left(-\frac{E}{kT}\right) \times \left[1 + \frac{(l-1)s}{\beta} \times \int_{T_0}^{T} \exp\left(-\frac{E}{kT}\right) dT\right]^{-l/(l-1)} \quad (3)$$

In the equation, E is the activated energy or the deepness of the trap, n_0 is the density of charge captured in the trap when $t = 0$, which directly affects the intensity of thermoluminescence, k is the Boltzmann constant ($k = 1.38 \times 10^{-23}$ J/K), s is the frequency factor, l is the dynamic series, β is the heating rate, and $\beta = 4$ K/s. Table 1 shows the fitting result of the sample

Table 1. Thermoluminescence Fitting Parameters of BASO:0.3Eu^{2+},0.1Tm^{3+}

peak	E (eV)	s (s^{-1})	T_m (K)	n_0 (cm^{-3})	l
1	0.62	9.62×10^8	326	2.95×10^7	1.96
2	0.70	7.70×10^8	363	2.05×10^7	1.98

BASO:0.3Eu^{2+},0.1Tm^{3+}. The two-dimensional thermoluminescence curve can be fitted to break up into two thermoluminescence peaks. The low-temperature peak is located at 326 K. The corresponding trap deepness values are 0.62 and 0.70 eV. If the peak position of thermoluminescence is too low, the decay of persistent luminescence is very fast, and the time of duration is short. If the peak position of thermoluminescence is too high, the storage energy is difficult to be released in room temperature, and the persistent luminescence is weak. Thus, the thermoluminescence peak position of the better persistent luminescence material should be in the range of 320 and 393 K (about 0.65 eV).[10]

There are two thermoluminescence peaks located at 326 and 363 K to the sample BASO:0.3Eu^{2+},0.1Tm^{3+}. Thus, the two thermoluminescence peaks both make contributions to the persistent luminescence property of the sample. Also, the thermoluminescence curve is a broad-band curve and can cover the temperature region from 300 to 450 K. This indicates that the distribution of traps in the material is wide. Generally, it is believed that the release rate of energy in the shallow trap is quick, the release rate of energy in the deep trap is slow, and the duration time is long. From Table 1, we can see that the density of charge carrier captured in the shallow trap and deep trap is basically close, which indicates that BASO:0.3Eu^{2+},0.1Tm^{3+} possesses not only the high intensity of persistent luminescence but also the long persistent luminescence duration time.

Figure 5a shows the two-dimensional thermoluminescence curves of BASO:0.3Eu^{2+},$y$$Tm^{3+}$ (y = 0, 0.05, 0.10, 0.20, 0.30, and 0.40). With the increase in Tm^{3+} concentration, the intensity of persistent luminescence increases gradually. When y = 0.10, the thermoluminescence curve reaches the maximum. After continuously adding Tm^{3+}, the intensity of thermoluminescence decreases with it. The possible reason may be the concentration quenching owing to the excessive Tm^{3+} concentration. The storage energy returns to the ground state in the form of non-radiative transitions. Besides, although the persistent luminescence of BASO:0.3Eu^{2+} can be detected, its persistent luminescence property is poor. The thermoluminescence curve shape of BASO:0.3Eu^{2+} is similar to that of BASO:0.3Eu^{2+},$y$$Tm^{3+}$, as shown in Figure 5a. Besides, with the addition of Tm^{3+} , the peak edge of thermoluminescence

DOI: 10.1021/acsomega.9b00180
ACS Omega 2019, 4, 6923−6930

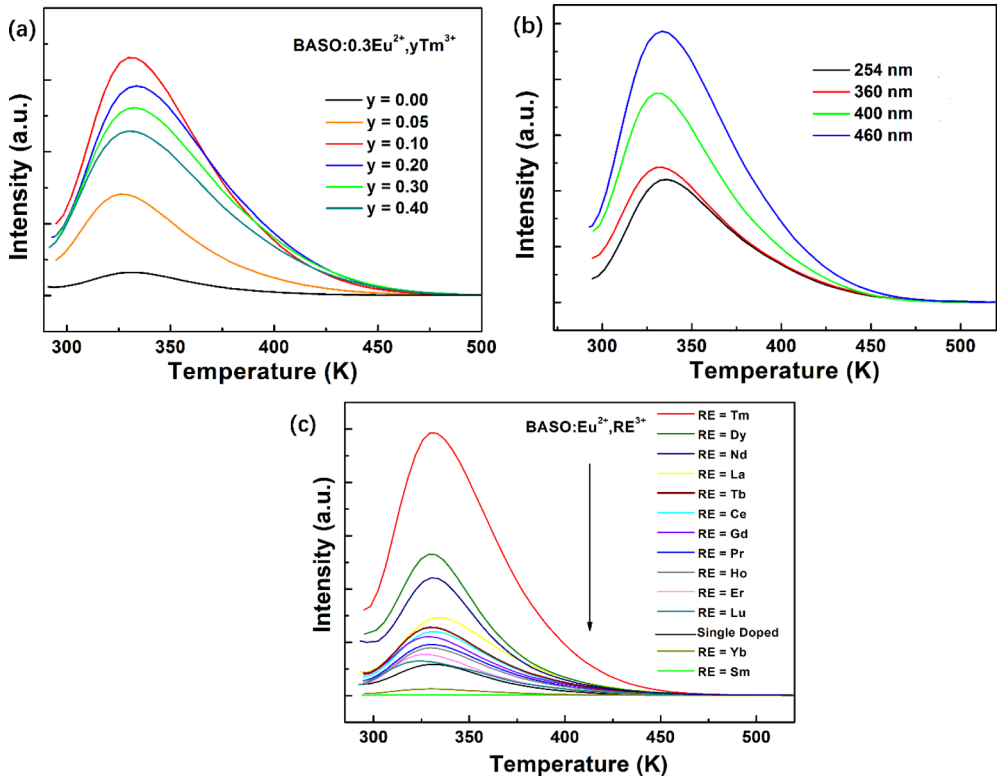

Figure 5. (a) Two-dimensional thermoluminescence curves of BASO:0.3Eu^{2+},yTm^{3+} (y = 0, 0.05, 0.10, 0.20, 0.30, and 0.40). (b) Thermoluminescence curves of BASO:0.3Eu^{2+},0.1Tm^{3+} at different excitation light. (c) Thermoluminescence curves of BASO:0.3Eu^{2+},0.1RE^{3+}.

slightly moves to the high temperature, which indicates that adding Tm^{3+} ions not only can increase the amount of traps in BASO:0.3Eu^{2+} but also can interact and increase the deepness of traps to some extent.

Figure 5b shows the thermoluminescence curves of BASO:0.3Eu^{2+},0.1Tm^{3+} at different excitation light. Generally, the wavelength of the excitation light is shorter, the energy is higher, and the rate of the energy storage is faster. However, the thermoluminescence intensity of the sample excited by a 250 nm light source is the lowest. With the increase in the excitation light wavelength, the intensity of thermoluminescence curve increases gradually. The thermoluminescence curve is the strongest at the excitation of a 460 nm light source. However, the main excitation peak of BASO:0.3Eu^{2+},0.1Tm^{3+} excitation spectra is located at around 380 nm. According to the analysis above, we can assume that the trap in the material has its own energy level distribution, and the lowest trap level must be lower than the bottom level of the d band of Eu^{2+} in the material, so that the persistent luminescence property of the sample is better when excited by the blue light with lower energy.

In the process of the preparation of BASO:Eu^{2+},Tm^{3+}, the mixture of rare-earth ions and the change in the matrix both result in the generation of the defects. Because the ionic radii of Eu^{2+} and Tm^{3+} are more close to Ba^{2+}, the doping Eu^{2+} and Tm^{3+} ions in the lattice mainly substitute the position of Ba^{2+}. The ionic solid-phase reaction chemical formula of the Eu^{2+} and Tm^{3+} ions doped into the matrix is as follows:

$$(13.35 - x - y)BaCO_3 + Al_2O_3 + SiO_2 + 0.5xEu_2O_3 + 0.5zTm_2O_3 + 0.5xCO \rightarrow Ba_{(13.35-x-y)}Al_{30.7}Si_{5.3}O_{70}: xEu^{\times}_{Ba}, yTm^{\bullet}_{Ba} + 0.5zV''_{Ba} + (13.35 - 0.5x - y)CO_2 \quad (4)$$

Eu^{2+} doped into the lattice is a kind of equivalent substitution process. The lattice defect $Eu^{\times}_{Ba}$ is generated after the substitution of Ba^{2+} without charge. Tm^{3+} that entered the lattice is a kind of non-equivalent substitution process. Point defect $Tm^{\bullet}_{Ba}$ is generated after the substitution of Ba^{2+} with positive charge. To balance the charge of the crystal, one Ba ion vacancy V''_{Ba} with two negative charges will be generated when two Tm^{3+} ions enter the lattice. Reducing the synthetic atmosphere makes some O ions react with the reducing gas and break away. Thus, there exists O ion vacancy $V^{\bullet\bullet}_{O}$ in the synthetic material.[26] $Eu^{\times}_{Ba}$ is electrically neutral. Tm^{3+} ($Tm^{\bullet}_{Ba}$) bears one positive charge. V''_{Ba} bears two negative charges. $V^{\bullet\bullet}_{O}$ bears two positive charges. Eu^{2+}, as the luminescent center in $Eu^{\times}_{Ba}$, mainly affects the photoluminescence property and persistent luminescence color of the material. V''_{Ba} bears two negative charges, which can act as the vacancy trap in the material. Owing to the positive charge of Tm^{3+} ($Tm^{\bullet}_{Ba}$) and $V^{\bullet\bullet}_{O}$ defects, they are able to serve as the electron capture trap.

Persistent Luminescence Mechanism for BASO:Eu^{2+},Tm^{3+}. We have already analyzed the existing defects in BASO:Eu^{2+},Tm^{3+} in detail. To understand the function of different kinds of defects to the persistent luminescence of materials better, we prepared the other co-doped trivalent rare-earth ion series sample BASO:0.3Eu^{2+},0.1RE^{3+} and characterized them with the thermoluminescence curve. In Figure 5c,

DOI: 10.1021/acsomega.9b00180
ACS Omega 2019, 4, 6923−6930

after co-doping Tm^{3+}, Dy^{3+}, Nd^{3+}, La^{3+}, Tb^{3+}, Ce^{3+}, Gd^{3+}, Pr^{3+}, Ho^{3+}, Er^{3+}, and Lu^{3+} ions, the intensities of thermoluminescence all increase. In the above order, the influence of trivalent rare-earth ions to the persistent luminescence property of BASO:0.3Eu^{2+} decreases gradually. After co-doping Sm^{3+} and Yb^{3+} ions, the thermoluminescence intensity of the sample decreases on the contrary. Besides, a single-doped sample also possesses a persistent luminescence phenomenon. This indicated that traps exist in BASO:0.3Eu^{2+}, which can store energy. Therefore, the energy storage center of the sample may be generated by V''_{Ba} and $V_O^{\bullet\bullet}$ in the lattice.

The amount of V''_{Ba} will be improved in the sample after adding RE^{3+} ions. Thus, the improvement of the persistent luminescence intensity is possibly due to the increase in the amount of V''_{Ba}. However, different RE^{3+} ions affect the persistent luminescence of BASO:0.3Eu^{2+} differently. Besides, the addition of Sm^{3+} and Yb^{3+} decreases the thermoluminescence intensity of the material, which indicates that the increase in the amount of V''_{Ba} is not the main factor that affects thermoluminescence. Therefore, it can be deduced that Tm^{3+} ions interact with the defects in the material. $V_O^{\bullet\bullet}$ and Tm^{3+} in the material can both act as the electron trap. Tm^{3+} can improve the ability of the electron capture in the material, thus improve its persistent luminescence intensity. By observing the thermoluminescence intensity changing law (Figure 5c), we discover that the influence of RE^{3+} ions on the thermoluminescence intensity is closely related to the optical electronegativity of the rare-earth ions. The so-called optical electronegativity is the parameter of the ability that rare-earth ions attract electrons. The electronegativity is bigger, and the ability to attract electron is stronger. On the contrary, the ability to attract electron is smaller. Co-doped RE^{3+} ions can interact with other defects to capture an excited electron. Thus, the co-doped RE^{3+} ions can improve the energy storage ability of the material and then improve the persistent luminescence property of the material. Tm^{3+}, Dy^{3+}, and Nd^{3+} ions improve the thermoluminescence intensity of the material drastically. The improvement of La^{3+}, Tb^{3+}, Ce^{3+}, Gd^{3+}, Pr^{3+}, Ho^{3+}, Er^{3+}, Yb^{3+}, and Lu^{3+} ions to the thermoluminescence intensity of the material is not obvious. After adding Sm^{3+} and Yb^{3+} ions, the thermoluminescence intensity of the material decreases on the contrary. This indicates that RE^{3+} ions can improve the persistent luminescence intensity of the material within its optical electronegativity in an appropriate range. If the optical electronegativity is too small, then it cannot capture an electron with other defects effectively. If the optical electronegativity is too large, then the ability of absorption of electron is too strong to release the captured electron in the material. In this material, Sm^{3+} and Yb^{3+} ions possess large optical electronegativity. The captured electron cannot be released effectively, which leads to the decrease of thermoluminescence intensity in BASO:0.3Eu^{2+}. The optical electronegativity of La^{3+}, Tb^{3+}, Ce^{3+}, Gd^{3+}, Pr^{3+}, Ho^{3+}, Er^{3+}, Yb^{3+}, and Lu^{3+} ions is too small. They obviously cannot improve the thermoluminescence intensity of the sample.

We propose a persistent luminescence mechanism for BASO:Eu^{2+},Tm^{3+}, as shown in Figure 6. After Eu^{2+} is activated by the light source, electrons transition from the ground state 4f orbital to the 5d orbital and become excited electrons. Then, they are captured by the electron trap. The captured electrons are activated again to the 5d orbital of Eu^{2+} ion under the action of temperature. The electrons in the 5d orbital transition to the 4f orbital and generate yellow persistent luminescence. According to the discussion above, the intensity of persistent luminescence excited by a 460 nm light source is higher than the intensity excited by a 254 nm light source. Besides, the energy of a 460 nm light source is lower than the conduction band. This indicates that the captured excited electrons do not transmit by the conduction band but may directly transmit from the 5d orbital to deflect the energy level by the tunneling effect. Also, by thermal activation, the captured electrons directly transmit to the Eu^{2+} luminescence center without passing the conduction band. Thus, the sample irradiated under the light source with lower energy can generate stronger persistent luminescence.

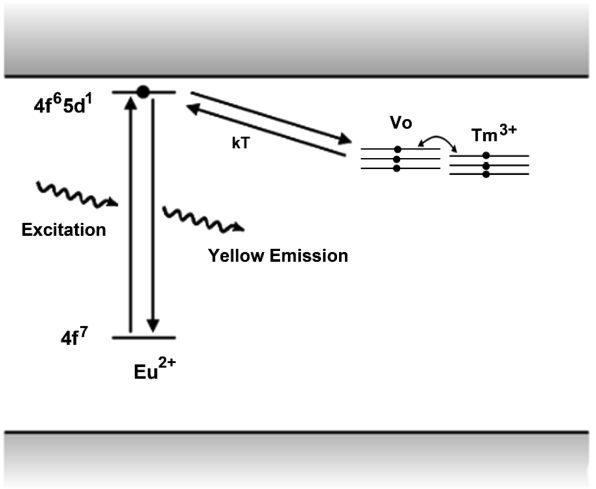

Figure 6. Schematic graph of persistent luminescence mechanism for BASO:Eu^{2+},Tm^{3+}.

CONCLUSIONS

By the high-temperature solid-state method, we synthesized a yellow long persistent luminescence phosphor $Ba_{13.35}Al_{30.7}Si_{5.3}O_{70}$:$Eu^{2+}$,$Tm^{3+}$. The Rietveld analysis shows that $Ba_{13.35}Al_{30.7}Si_{5.3}O_{70}$:$Eu^{2+}$,$Tm^{3+}$ has the same orthorhombic crystal structure with $Ba_{13.35}Al_{30.7}Si_{5.3}O_{70}$. The $Ba_{13.35}Al_{30.7}Si_{5.3}O_{70}$:$Eu^{2+}$,$Tm^{3+}$ phosphors can be efficiently activated by sunlight and ultraviolet light and exhibited excellent yellow long persistent luminescence. The persistent luminescence can be observed after 8 h in a dark room. By thermoluminescence spectra, we realize the trap distribution of $Ba_{13.35}Al_{30.7}Si_{5.3}O_{70}$:$Eu^{2+}$,$Tm^{3+}$. Also, the corresponding mechanism of persistent luminescence has been illustrated.

EXPERIMENTAL SECTION

Preparation of the Sample. All the samples in this paper were prepared by a high-temperature solid-phase reaction. The raw materials needed were $BaCO_3$ (A.R.), Al_2O_3 (A.R.), SiO_2 (A.R.), Eu_2O_3 (99.99%), H_3BO_3, and Re_xO_y (RE = La, Ce, Pr, Nd, Sm, Gd, Tb, Dy, Ho, Er, Tm, Yb, and Lu) (99.99%). The chemical composition of the sample was $Ba_{(13.35-x-y)}Al_{30.7}Si_{5.3}O_{70}$:$xEu^{2+}$,$yRE^{3+}$ (denoted as BASO:x-Eu^{2+},yRE^{3+}, where x and y are the molar fractions of the dopant).

The abovementioned material as the stoichiometric ratio of the target compound was weighed accurately. H_3BO_3 (5 mol % of Ba element) was added as the co-solvent. The weighing raw material was placed into an agate mortar, ground, and blended for 15 min. The intensively mixed raw material was placed into

DOI: 10.1021/acsomega.9b00180
ACS Omega 2019, 4, 6923−6930

an alumina crucible. Then, the crucible with the sample was put into a big crucible filled with activated carbon. The reaction temperature was 1653 K. The sample was calcined in the furnace in 1653 K for 6 h. After the reaction, the sample was cooled to room temperature in the furnace. The obtained samples were ground into powder for the following measurement.

Measurements and Characterization. Powder X-ray diffraction measurements were performed on a Bruker D8 focus diffractometer at a scanning rate of $2°\cdot min^{-1}$ in the 2θ range from 10° to 90°, with graphite-monochromatized Cu Kα_1 radiation (λ = 0.15405 nm) operating at 40 kV and 40 mA. The photoluminescence (PL) and photoluminescence excitation (PLE) spectra of the obtained materials were recorded by a Hitachi F-7000 spectrophotometer equipped with a 150 W xenon lamp as the excitation source. The persistent luminescence spectra and intensity decay curves were also measured using the same instrument after the samples were irradiated under 365 nm UV light for 2 min. The thermoluminescence curves were measured with a homemade spectrum instrument mainly consisting of a CCD detector and a heating apparatus. The sample was placed in a homemade sample holder and heated from room temperature to 413 K at a speed of 4 $K\cdot s^{-1}$. The sun irradiation experiments were carried out in a sunny day (11 a.m.), and the photographs were taken in a dark room.

AUTHOR INFORMATION

Corresponding Authors

*E-mail: jiayonglei17@nudt.edu.cn (Y.J.).
*E-mail: qutianliang@nudt.edu.cn (T.Q.).

ORCID

Yonglei Jia: 0000-0003-3323-3890

Notes

The authors declare no competing financial interest.

ACKNOWLEDGMENTS

This work was supported by the National Natural Science Foundation of China (grant nos. 11304384 and 61575220).

REFERENCES

(1) Hirata, S.; Vacha, M. White Afterglow Room-Temperature Emission from an Isolated Single Aromatic Unit under Ambient Condition. *Adv. Opt. Mater.* **2017**, *5*, 1600996.

(2) Clabau, F.; Rocquefelte, X.; Jobic, S.; Deniard, P.; Whangbo, M.-H.; Garcia, A.; Le Mercier, T. Mechanism of Phosphorescence Appropriate for the Long-Lasting Phosphors Eu^{2+}-Doped $SrAl_2O_4$ with Codopants Dy^{3+} and B^{3+}. *Chem. Mater.* **2005**, *17*, 3904−3912.

(3) Maldiney, T.; Lecointre, A.; Viana, B.; Bessière, A.; Bessodes, M.; Gourier, D.; Richard, C.; Scherman, D. Controlling Electron Trap Depth To Enhance Optical Properties of Persistent Luminescence Nanoparticles for In Vivo Imaging. *J. Am. Chem. Soc.* **2011**, *133*, 11810−11815.

(4) Maldiney, T.; Bessière, A.; Seguin, J.; Teston, E.; Sharma, S. K.; Viana, B.; Bos, A. J. J.; Dorenbos, P.; Bessodes, M.; Gourier, D.; Scherman, D.; Richard, C. The in vivo activation of persistent nanophosphors for optical imaging of vascularization, tumours and grafted cells. *Nat. Mater.* **2014**, *13*, 418.

(5) Matsuzawa, T.; Aoki, Y.; Takeuchi, N.; Murayama, Y. A New Long Phosphorescent Phosphor with High Brightness, $SrAl_2O_4$: Eu^{2+}, Dy^{3+}. *J. Electrochem. Soc.* **1996**, *143*, 2670−2673.

(6) Zou, R.; Gong, R.; Shi, J.; Jiao, J.; Wong, K.-L.; Zhang, H.; Wang, J.; Su, Q. Magnetic-NIR Persistent Luminescent Dual-Modal ZGOCS@MSNs@Gd_2O_3 Core−Shell Nanoprobes For In Vivo Imaging. *Chem. Mater.* **2017**, *29*, 3938−3946.

(7) Zou, R.; Huang, J.; Shi, J.; Huang, L.; Zhang, X.; Wong, K.-L.; Zhang, H.; Jin, D.; Wang, J.; Su, Q. Silica shell-assisted synthetic route for mono-disperse persistent nanophosphors with enhanced in vivo recharged near-infrared persistent luminescence. *Nano Res.* **2017**, *10*, 2070−2082.

(8) Le Masne de Chermont, Q.; Chanéac, C.; Seguin, J.; Pellé, F.; Maîtrejean, S.; Jolivet, J.-P.; Gourier, D.; Bessodes, M.; Scherman, D. Nanoprobes with near-infrared persistent luminescence for in vivo imaging. *PNAS* **2007**, *104*, 9266−9271.

(9) Pan, Z.; Lu, Y.-Y.; Liu, F. Sunlight-activated long-persistent luminescence in the near-infrared from Cr^{3+}-doped zinc gallogermanates. *Nat. Mater.* **2012**, *11*, 58−63.

(10) Van den Eeckhout, K.; Smet, P. F.; Poelman, D. Persistent Luminescence in Eu^{2+}-Doped Compounds: A Review. *Materials* **2010**, *3*, 2536.

(11) Wang, P.; Xu, X.; Qiu, J.; Yu, X.; Wang, Q. Effects of Er^{3+} doping on the long-persistent luminescence properties of $Ba_4(Si_3O_8)_2$:Eu^{2+} phosphor. *Opt. Mater.* **2014**, *36*, 1826−1829.

(12) Chiari, G.; Gazzoni, G.; Craig, J. R.; Gibbs, G. V.; Louisnathan, S. J. Two independent refinements of the structure of paracelsian, $BaAl_2Si_2O_8$. *Am. Mineral.* **1985**, *70*, 969−974.

(13) Smith, J. V. The crystal structure of paracelsian, $BaAl_2Si_2O_8$. *Acta Crystallogr.* **1953**, *6*, 613−620.

(14) Clabau, F.; Garcia, A.; Bonville, P.; Gonbeau, D.; Le Mercier, T.; Deniard, P.; Jobic, S. Fluorescence and phosphorescence properties of the low temperature forms of the $MAl_2Si_2O_8$:Eu^{2+} (M=Ca, Sr, Ba) compounds. *J. Solid State Chem.* **2008**, *181*, 1456−1461.

(15) Pawade, V. B.; Dhoble, S. J. Trap depth and Dy^{3+} luminescence in $BaAl_2Si_2O_8$ phosphor. *J. Lumin.* **2014**, *145*, 626−630.

(16) Rief, A.; Kubel, F.; Hagemann, H. Optical and Structural Properties of a Eu(II)-Doped Silico-aluminate with Channel Structure and Partial Site Occupation. *Zeitschrift für Naturforschung B* **2007**, *62*, 1535.

(17) Rodríguez Burbano, D. C.; Sharma, S. K.; Dorenbos, P.; Viana, B.; Capobianco, J. A. Persistent and Photostimulated Red Emission in CaS:Eu^{2+},Dy^{3+} Nanophosphors. *Adv. Opt. Mater.* **2015**, *3*, 551−557.

(18) Gong, Y.; Wang, Y.; Li, Y.; Xu, X.; Zeng, W. Fluorescence and phosphorescence properties of new long-lasting phosphor $Ba_4(Si_3O_8)_2$:Eu^{2+}, Dy^{3+}. *Opt. Express* **2011**, *19*, 4310−4315.

(19) Van Uitert, L. G. An empirical relation fitting the position in energy of the lower d-band edge for Eu^{2+} OR Ce^{3+} in various compounds. *J. Lumin.* **1984**, *29*, 1−9.

(20) Sun, W.; Li, H.; Zheng, B.; Pang, R.; Jiang, L.; Zhang, S.; Li, C. Electronic structure and photoluminescence properties of a novel single-phased color tunable phosphor $KAlGeO_4$:Bi^{3+},Eu^{3+} for WLEDs. *J. Alloys Compd.* **2019**, *774*, 477−486.

(21) Jia, D.; Jia, W.; Evans, D. R.; Dennis, W. M.; Liu, H.; Zhu, J.; Yen, W. M. Trapping processes in CaS:Eu^{2+},Tm^{3+}. *J. Appl. Phys.* **2000**, *88*, 3402−3407.

(22) Uchiyama, T.; Tomaru, T.; Tobar, M. E.; Tatsumi, D.; Miyoki, S.; Ohashi, M.; Kuroda, K.; Suzuki, T.; Sato, N.; Haruyama, T.; Yamamoto, A.; Shintomi, T. Mechanical quality factor of a cryogenic sapphire test mass for gravitational wave detectors. *Phys. Lett. A* **1999**, *261*, 5−11.

(23) Gutiérrez-Martín, F.; Fernández-Martinez, F.; Díaz, P.; Colón, C.; Alonso-Medina, A. Persistent UV phosphors for application in photo catalysis. *J. Alloys Compd.* **2010**, *501*, 193−197.

(24) Lin, H.; Bai, G.; Yu, T.; Tsang, M. K.; Zhang, Q.; Hao, J. Site Occupancy and Near-Infrared Luminescence in $Ca_3Ga_2Ge_3O_{12}$: Cr^{3+} Persistent Phosphor. *Adv. Opt. Mater.* **2017**, *5*, 1700227.

(25) McKeever, S. *Thermoluminescence of Solids*. Cambridge University Press: 1988.

(26) Yang, X.; Tiam, T. S.; Yu, X.; Demir, H. V.; Sun, X. W. Europium (II)-Doped Microporous Zeolite Derivatives with Enhanced Photoluminescence by Isolating Active Luminescence Centers. *ACS Appl. Mater. Interfaces* **2011**, *3*, 4431−4436.

DOI: 10.1021/acsomega.9b00180
ACS Omega 2019, 4, 6923−6930